Design of a Triple-band Microstrip Bandpass Filter with Wide Harmonic Suppression Based on Stepped-impedance Resonators

Thaweewong Akkaralaertsest[1], Suttee Tubtongdee[1], Adisorn Sirikham[1], Jessada Konpang[1 *] and Nattapong Intarawiset[2]

[1] Department of Electrical and Telecommunication Engineering, Faculty of Engineering, Rajamangala University of Technology Krungthep
2 Nanglingee Road, Thungmahamek, Sathorn, Bangkok, Thailand, 10120

[2] Department of Industrial Education and Technology, Faculty of Engineering, Rajamangala University of Technology Lanna
128 Huay Kaew Road, Muang, Chiang Mai, Thailand, 50300

[*]Corresponding Author: jessada.k@mail.rmutk.ac.th Phone Number: 06-4569-7560

Received: 11 August 2022, Revised: 8 November 2022, Accepted: 9 November 2022

Abstract

This paper presents a triple-band microstrip bandpass filter with a broad harmonic suppression based on stepped-impedance resonators. This stepped-impedance resonator structure reduces the microstrip open-loop halfwave length resonator filter's circuit size. The straightforward design technique is based on three independently different bandpass filters combined in the triple-band filter form. The three independent filters are designed at 900, 1800 MHz, and 2450 MHz center frequency. The excited coupling feeders have also produced the transmission zeros between each filter. An acquirement of their transmission zeros between each passband results in a sharp out-off band rejection. Simulated and measured results show a remarkable agreement that the insertion losses /S_{21}/ inside three passbands are less than 2.1 dB.

Keywords: Triple-band, microstrip bandpass filter, open-loop stepped-impedance, microwave filter.

1. Introduction

Recently, the advance of Radio Frequency (RF)/microwave communication requires a high quality of transmitting and receiving the signal with a small circuit component for multi-channel paths. Dual-band and multiband filters play an essential role in meeting these requirements of multiband services. Various methods are suggested for designing dual- and triple-band bandpass filters (BPFs). Microstrip dual- and triple-band-based microstrip structures are more flexible circuit designs with low loss, small circuit size, and lightweight circuit layout filters [1]. The microwave dual-band filters are highly desirable in wireless communication systems and are discussed in many research works. A dual-band bandpass filter has been presented in [2]; however, the configuration still occupies a large area as a cascade connection of a wide-band bandpass filter and a band-stop filter. Dual-band filter design which is tunable dual-band resonators, presented with

stepped-impedance transmission-line sections [3]. Cross-coupled filters with a dual-passband response are designed as compact miniaturized hairpin resonators, which are elliptic function type designs [4]. Controllable fractional bandwidths of dual-band bandpass filters are constructed by multiple stepped-impedance resonators and parallel-coupled microstrip lines [5]. Dual-band bandpass filters (BPFs) with a simple design method are suggested using two independently controllable bandwidths [6]. Half-mode substrate integrated waveguide (HMSIW) resonators are introduced as a compact dual-band filter using the quasi-TEM mode and the TE102 mode of the novel HMSIW resonator [7]. A Dual-band bandpass filter utilizing an asymmetrical stepped-impedance resonator is designed as a high-selectivity response for a dual-band filter [8]. The microstrip filters based on stepped-impedance resonators have a compact size and high signal performance resonator structure. Two adjacent coupling half-wavelength stepped-impedance resonators (SIRs) with a defective ground structure (DGS) is presented as dual-band bandpass filter [9]. Meandering stepped impedance resonators (SIRs) exhibit a size reduction in a miniaturized dual-band narrow bandpass filter (BPF) [10]. A coupling configuration of the stepped impedance resonator (SIR) has been introduced to design dual-band bandpass filters with a small circuit size [11]. Dual- and triple-band characteristics are achieved using Coupling structures with both Chebyshev and quasi-elliptic frequency responses [12].

Moreover, the dual- and triple-band filters are fabricated on various materials such as metal cavities and dielectric resonators. In [13], the dual- and triple-band tunable filters in a single cavity are achieved by putting two or three identical sets of metal-post pairs. The manifold approach is used to design new multiband waveguide filters as in [14]. Triple-band dielectric resonator in a metallic cavity is represented in [15]. However, the design structure based on metallic waveguides is still in large constructions. A triple-band filter has been proposed in [16] with a half-wavelength resonator to design the miniaturizing planar circuit. A triple-band high temperature superconducting (HTS) filter using coupled-line stepped impedance-resonator (C-SIR) has been proposed in [17]. In [18], planar filters are designed by using a multi-stub-loaded differential-mode. Low profile and lightweight structures can be designed by substrate integrated waveguide (SIW), with a low-cost structure while maintaining good performance. SIW- are represented in [19]-[21] for dual- and triple-band resonator filters. All of these multiband filters are focused on various materials and structures. However, microstrip RF/microwave filters provide a flexible design with a small circuit, low loss, and low complexity designs.

This paper presents a triple-band microstrip bandpass filter with a wide harmonic suppression based on stepped-impedance resonators to offer low loss, low cost, and good rejection responses. The independent three resonator filters are combined using the same coupling feeder, which helps reduce tuning resonant frequencies.

2. Materials and Methods

The basis of the stepped-resonator filter design can be explained in this section. Microstrip stepped-impedance resonator can be represented in the form of a half-wavelength shown in figure 1(a). The stepped-impedance resonator configuration consists of two lines of different characteristic impedance Z_1 and Z_2, admittance Y_1 and Y_2, and electrical lengths

θ_1 and θ_2, respectively. The *ABCD* matrix can explain the non-uniform stepped impedance structure like the following matrix.

$$\begin{bmatrix} A & B \\ C & D \end{bmatrix} = \begin{bmatrix} \cos\theta_2 & jZ_1\sin\theta_2 \\ j\frac{\sin\theta_2}{Z_2} & \cos\theta_2 \end{bmatrix} \begin{bmatrix} \cos 2\theta_1 & jZ_2\sin\theta_1 \\ j\frac{\sin 2\theta_1}{Z_1} & \cos\theta_1 \end{bmatrix} \begin{bmatrix} \cos\theta_2 & jZ_1\sin\theta_2 \\ j\frac{\sin\theta_2}{Z_2} & \cos\theta_2 \end{bmatrix} \quad (1)$$

The input admittance Y_{in} of the symmetric stepped-impedance can be expressed as;

$$Y_{in}=jY_2\frac{2(K\tan\theta_1+\tan\theta_2)\cdot(K-\tan\theta_1\cdot\tan\theta_2)}{K(1-\tan^2\theta_1)(1-\tan^2\theta_2)-2(1+K^2)\tan\theta_1\cdot\tan\theta_2} \quad (2)$$

Where *K* is the ratio of characteristic impedances of Z_2/Z_1=(*Rz* <1). At resonant condition, Y_{in} is zero, then the first mode and second mode frequencies of the stepped-impedance resonator are explained in [22].

$$\tan\theta_1 = Rz\cot\theta_2 \quad (at\ f=f_1) \quad (3)$$

Where R_z is the ratio of characteristic impedance Z_2 to Z_1, and the electrical length of the resonator is denoted as θ_1 and θ_2 for the first mode (f_1). The second mode (f_2) can be calculated as

$$\cot\theta_1 = -R_z\cot\theta_2 \quad (at\ f=f_2) \quad (4)$$

When (R_z <1), the resonator has a small size and wide stopband by selecting a ratio value of R_z.

The triple-band stepped-impedance resonator can achieve by using the filter design based on an independent filter. Firstly, the filter is designed independently at the center frequency of 900 MHz, 1800 MHz, and 2450 MHz. Based on the coupling method, the input/output external quality factors, Q_e, and the internal coupling coefficient between the adjacent resonators, Kij can be expressed in the following equation.

$$Q_e = \frac{g_0 g_1}{FBW} \quad (5)$$

$$K_{ij} = \frac{-FBW}{\sqrt{g_0 g_1}} \quad (6)$$

Where *FBW* is the fractional bandwidth of the bandpass filter, element values g_0 and g_2 are 1.0, and g_1 is 1.4142 for Chebyshev lowpass filter elements [23]. The proposed triple-band filter for the center frequencies of 900MHz, 1800MHz, and 2450MHz with fractional bandwidth (*FBW*=6.6% at 900 MHz, 4.4% at 1800 MHz, and 3.5% at 2450 MHz), respectively. The corresponding external quality factors (Q_e) are 21.23 for the first band, 31.85 for the second band, and 48.49 for the third band. The coupling coefficient K_{12} is 0.046 for fundamental resonant frequency f_1 = 900 MHz. The coupling coefficient K_{12} is 0.037 for the first mode f_1 = 1800 MHz, and K_{12} is 0.029 at 2450 MHz, respectively.

A beginning design for the miniaturization of the filter structure is used to be the beginning structure of these triple-band stepped-impedance resonator filters, as shown in Fig. 1(b). Typically, a symmetric feeder placed near the center of the resonator has no attenuation poles. In contrast, an asymmetric feeder, including the feed placed near the resonator's edge, has two attenuation poles beside the passband, which has sharp cutoff rejection near the passband. However, the feeding position is shown in Fig. 1(b) still has two attenuation poles between the lower side- and upper-sideband. Besides, the wide harmonic suppression can be improved at the upper side-band. With the help of topology in Fig. 1(b) and the frequency response in Fig. 1 (c), the location of the feed line (t) can be selected to meet the high performance of wide harmonic suppression on the upper side-band of the operating frequency band. Harmonic suppression is reduced by adjusting distance (t) from the beginning point of the center (*t*=0) to (*t*=20 mm) of the

coupling feed line, as plotted in Fig. 1(c). It has been found that the harmonic level is less than -20 dB when TZs are located between the passband filter. The relationship between the external coupling factors (Q_e) and the gap (g) is shown in Fig. 1(d). The coupling coefficient (K_{ij}) is depicted in Fig.1 (e).

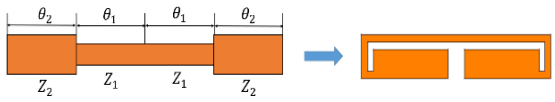

Fig. 1 (a) Basic layout of the stepped-impedance resonator (Rz<1)

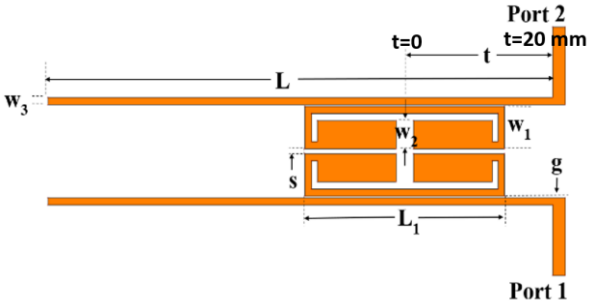

Fig. 1 (b) topology of the filter by changing feeding location

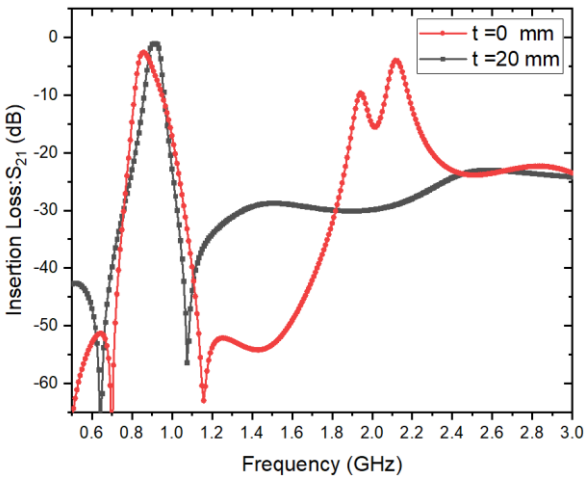

Fig. 1 (c) TZs and wide-band frequency response

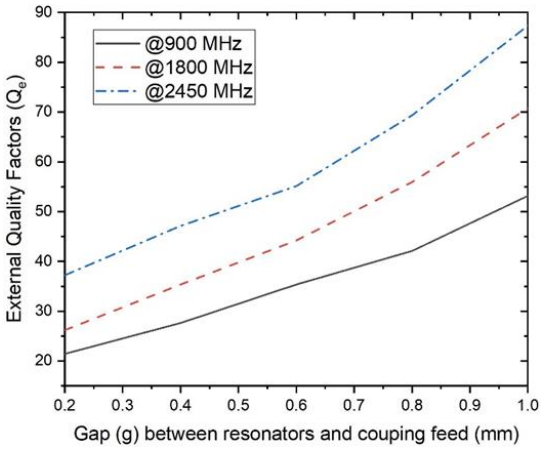

Fig. 1 (d) external coupling factors (Q_e)

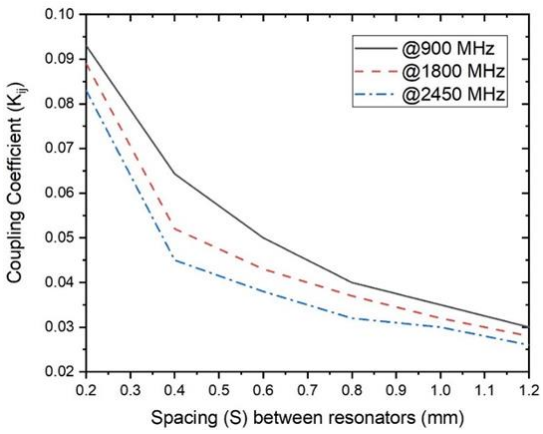

Fig. 1 (e) coupling coefficient (K_{ij})

3. Results and Discussion

3.1 Dual-band open-loop stepped-impedance resonator filter design

The filter was designed separately from each other and then combined to form dual-band and triple-band, respectively, to demonstrate the dual-band as the first example in this section. The input/output (I/O) structure is used to couple between microstrip lines and stepped-impedance resonators. An example of a dual-band resonator filter is operating at the frequency of 900 MHz, and the second resonator filter is designed at the operational frequency of 1800 MHz. The IE3D program is used to develop the filters with dielectric

substrate height h= 1.27mm and relative dielectric constant ε_r =6.15.

Fig. 2 (a) shows the dual-band filter's schematic structure, designed in the form of two bandpass filters independently. The dimensions of the filters are listed in Table 1.

Table 1 The sizes of stepped-impedance dual-band and triple-band resonator

Dimensions	F1=900 MHZ	F2=1800 MHZ	F3=2450 MHZ
Resonator width (w_1)	6mm	5.8mm	5.4mm
Stepped-impedance width (w_2)	4mm	4mm	4.29mm
Feed width (w_3)			
The gap between coupling-feed and	1mm	1mm	1mm
stepped-impedance resonator (g)	0.25mm	0.31mm	0.6mm
Spacing between resonators(s)			
Feed length (L)			
Resonator length (L_1)			
Resonator length (L_2)	0.73mm	0.93mm	1.07mm
Resonator length (L_3)			
Distance between resonator filter (D_1)		75.13mm	
Distance between resonator filter (D_2)	29.67mm		
		14.4mm	
			9.6mm
	5.46mm	5.46mm	
		5.89 mm	5.89 mm

Moreover, Fig. 2(b) and 2(c) show the density of current flows on the resonator's metallic surface at the center frequencies of 900 MHz and 1800 MHz, respectively. When the dual-band operates in the first resonant filter (900 MHz), The current flows from the input port to the output port at its resonant frequency band at 900 MHz, not for the second band (1800 MHz). On the other hand, when the second resonant frequency band (1800 MHz) is operated, most electric current flows via the second resonator at its resonant frequency. The independent design can work adequately in its resonant frequency and cooperate very well when combining in the form of a dual-band filter.

The implementation of the dual-band second-order resonator filter is shown in Fig. 3(a). A circuit board plotter produces the dual-band filter prototype. The network analyzer is used to measure the reflection and insertion loss. The dual-band filter frequency response at 900 MHz and 1800 MHz is portrayed in Fig.3(b). The insertion loss in both frequency bands is better than 1.8 dB, and the passband's return loss is greater than 20 dB. The frequency responses demonstrate the emergence of the transmission zeros on both sides of the passband at 900 MHz and 1800 MHz, improving the filter performance. Most of the losses are due to the SMA connectors and fabrication process.

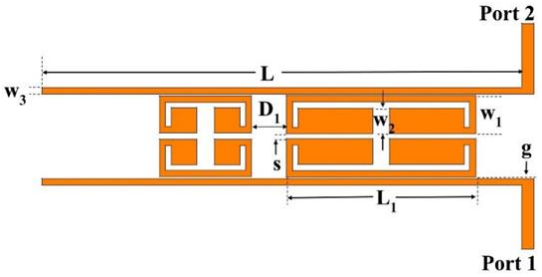

Fig. 2 (a) Layout of the dual-band filter at 900 and 1800 MHz

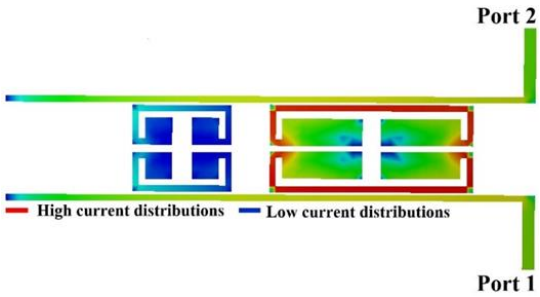

Fig. 2 (b) Current distribution of the dual-band at the first resonant frequency at 900 MHz

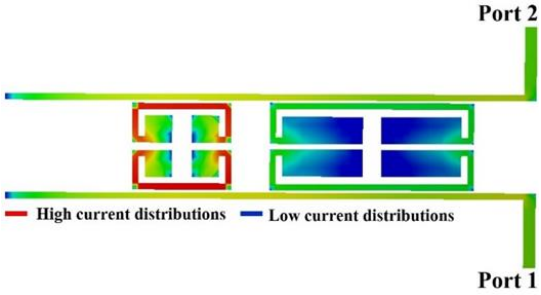

Fig. 2 (c) Current distribution of the dual-band at the second resonant frequency at 1800 MHz

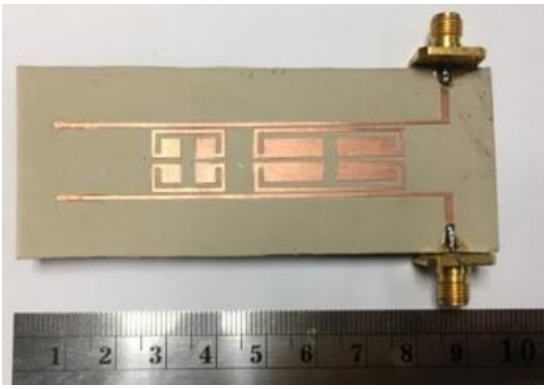

Fig. 3 (a) Fabricated dual-band filter at 900 and 1800 MHz

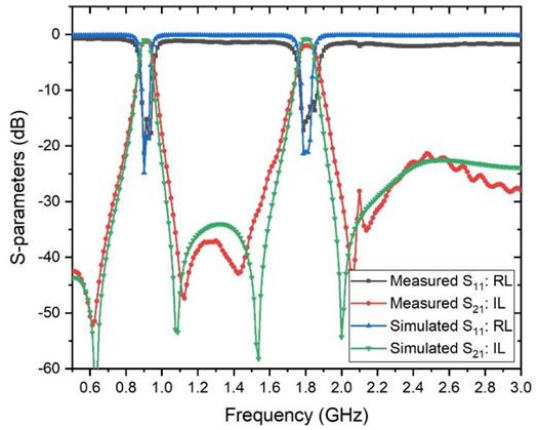

Fig. 3 (b) Frequency responses of the simulated results and the measured results.

Moreover, the principle of dual-band filter design can be proved by another dual-band frequency. Here, the dual-band filter at 1800 MHz and 2450 MHz can be introduced as another example. The dual-band filter structure was designed and simulated by the IE3D program, as shown in Fig. 4 (a). All dimensions are tabulated in table 1. Fig. 4(b) and 4(c) show the electric current distribution over the designed dual-band filter's strip conductor surface at the center frequencies of 1800 MHz and 2450 MHz, respectively.

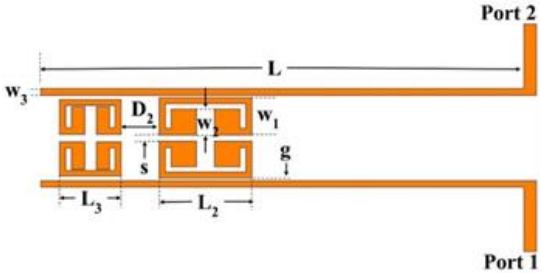

Fig. 4 (a) The filter at 1800 and 2450 MHz

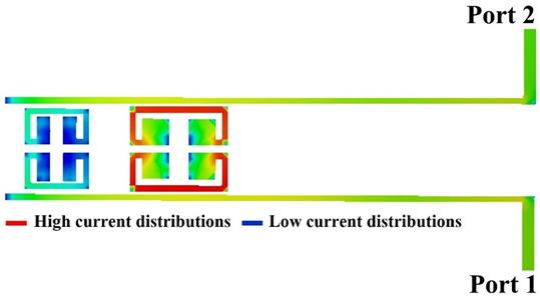

Fig. 4 (b) Distributed current at 1800 MHz

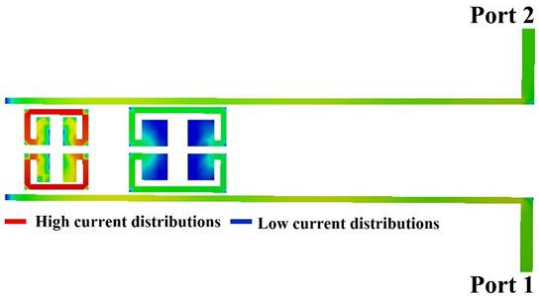

Fig. 4 (c) Distributed current at 2450 MHz

Fig. 5(a) displays the dual-band filter prototype at 1800 and 2450 MHz operating frequency, respectively. Fig. 5(b) shows the S-parameter responses of the dual-band filter in which the insertion loss inside the mid-band is better than 1.8 dB at 1800 MHz and 1.92 dB at 2450 MHz, respectively. The return losses are greater than 23 dB in both passbands. The filter exhibits two transmission zeros between the first- and the second frequency bands, improving the cut off rate of the filter response. The out-of-band rejections of both filters are more than 35 dB.

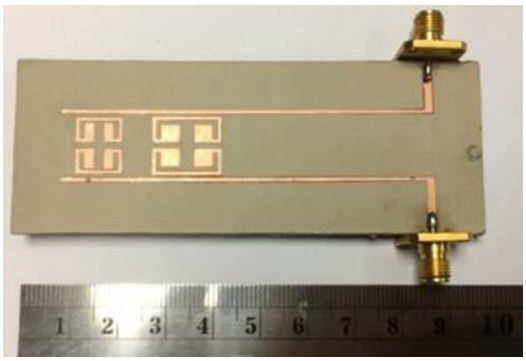

Fig. 5 (a) Fabricated dual-band filter at 1800 and 2450 MHz

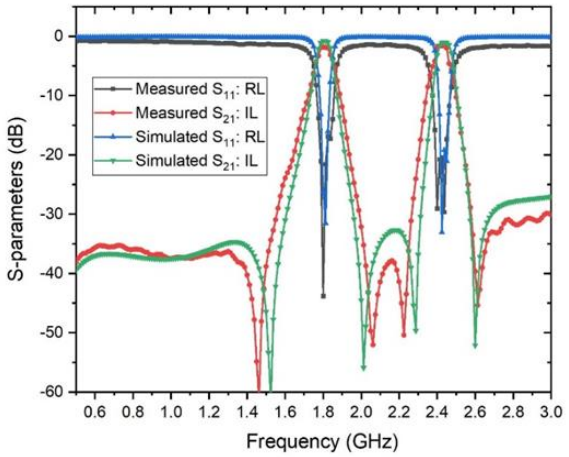

Fig. 5 (b) Frequency responses of the simulated results and the measured results

3.2. Triple-band stepped-resonator filter design

The triple-band filter geometry comprises three independent filters, as illustrated in Fig. 6(a). The design technique based on three filters with different frequencies is joined to form the triple-band filter. A coupled line is used to feed the signal between the input and output ports. To achieve the triple-band filter, the numerical simulator (IE3D program) can be used to simulate the current density and the S-parameters results. Fig.6(b), (c), and (d) show the distributed current flows of the designed triple-band filter at the center frequencies of 900 MHz, 1800 MHz, and 2450 MHz, respectively. All associated dimensions of the microstrip triple-band filter are detailed in Table 1.

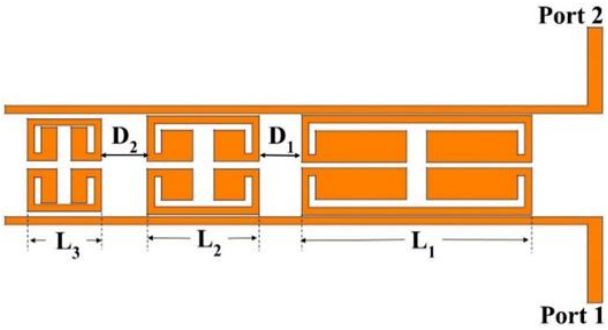

Fig. 6 (a) The triple-band resonator filter

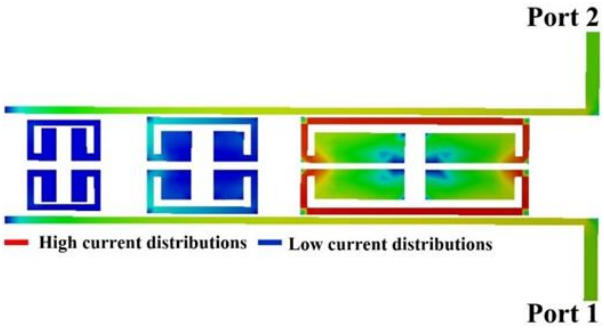

Fig. 6 (b) Distributed current at 900 MHz

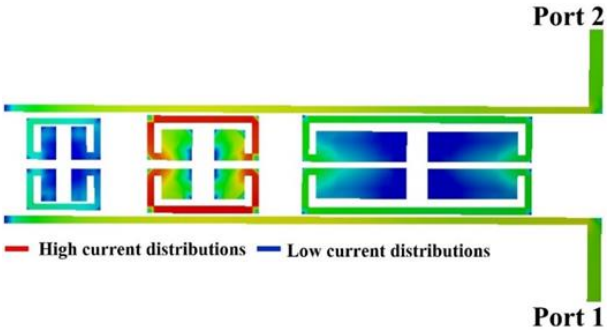

Fig. 6 (c) Distributed current at 1800 MHz

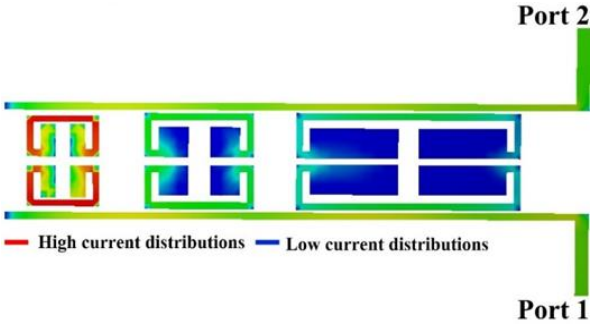

Fig. 6 (d) Distributed current at 2450 MHz

Table 2 The comparison with some previous triple-band bandpass filter (NG: Not Given)

Reference	Resonator type	Circuit size (mm)	Order	1st/2nd /3rd passbands (GHz)	IL (dB)
[14]	Waveguide resonator		3	11/11.5/12	0.6/2.6
[15]	Dielectric resonator	NG	3	3.8/4/4.2	0.36/0.41
[16]	Shorted-circuit stepped-impedance resonator		2	3.49/4.13/5.57	4.15/4.18/4.5
[17]	High-temperature superconducting filter using coupled-line stepped impedance resonator				
	Microstrip stepped impedance resonator	15X20	2	1.57/3.5/5.5	0.1/0.2/0.66
This work		80X30	2	0.9/1.8/2.45	1.75/1.8/1.92

A photograph of the fabricated triple-band filter is pictured in Fig. 7(a). The designed triple-band filter was also measured using an HP network analyzer. The measured performance is shown in Fig. 7(b). The microstrip triple-band is designed at the operational frequency of 900 MHz, 1800 MHz, and 2450 MHz with fractional bandwidth (FBW=6.6% at 900 MHz, 4.4% at 1800 MHz, and 3.5% at 2450 MHz), respectively. The passband insertion loss (IL) is less than 1.75 dB, 1.8 dB, and 1.92 dB. The return loss (RL) in three channels is better than 20 dB in the passband, as shown in Fig. 7(b). The losses are mainly attributed to the conductor loss of copper. The transmission zeros are located at 600 MHz, 1100 MHz, 1500 MHz, 2000 MHz, 2300 MHz, and 2550 MHz, improving the selectivity of the triple-band filter. The microstrip triple-band filter can enhance the out-of-band rejection of more than 35 dB between each band. The comparison with some reference triple-band filter has listed in Table 2.

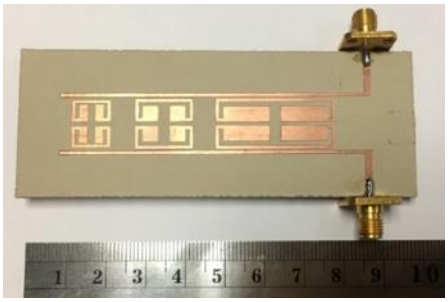

Fig. 7 (a) Fabricated triple-band filter at 900, 1800, and 2450 MHz, respectively

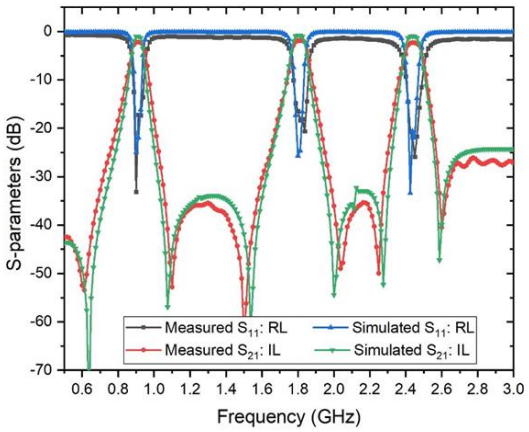

Fig. 7 (b) Frequency responses of the simulated results and the measured results

4. Conclusions

This work presents the ease of a triple-band bandpass filter utilizing stepped-impedance resonators with coupled-feed lines. A compact triple-band high-performance filter is easily realized to design with multi-frequency bands. The triple-band filter is achieved by using three independently resonant filters combined input/output coupled-feed lines. All six transmission zeros are also continuously produced. As a result, the triple-band filter's out-of-band rejection performance has been greatly improved by more than 35 dB. The measured insertion losses inside the three passbands are lower than 2 dB. Finally, this proposed triple-band filter can achieve ease of structure and fabrication process.

5. Acknowledgment

Authors gratefully acknowledge Department of Electrical and telecommunication engineering, Faculty of Engineering, Rajamangala University of Technology Krungthep and Department of industrial education and technology, Faculty of Engineering, Rajamangala University of Technology Lanna to support the research successfully.

6. References

[1] Pozar DM. Microwave engineering. John wiley & sons; 2011 Nov 22.

[2] Tsai LC, Hsue CW. Dual-band bandpass filters using equal-length coupled-serial-shunted lines and Z-transform technique. IEEE Transactions on Microwave Theory and Techniques. 2004 Apr 13;52(4):1111-7.

[3] Lee HM, Chen CR, Tsai CC, Tsai CM. Dual-band coupling and feed structure for microstrip filter design. In2004 IEEE MTT-S International Microwave Symposium Digest (IEEE Cat. No. 04CH37535) 2004 Jun 6 (Vol. 3, pp. 1971-1974). IEEE.

[4] Kuo JT, Cheng HS. Design of quasi-elliptic function filters with a dual-passband response. IEEE Microwave and Wireless Components Letters. 2004 Oct 4;14(10):472-4.

[5] Sun S, Zhu L. Coupling dispersion of parallel-coupled microstrip lines for dual-band filters with controllable fractional pass bandwidths. InIEEE MTT-S International Microwave Symposium Digest, 2005. 2005 Jun 17 (pp. 2195-2198). IEEE.

[6] Cho YH, Wang XG, Yun SW. Design of dual-band interdigital bandpass filters using both series and shunt resonators. IEEE microwave and wireless components letters. 2012 Feb 24;22(3):111-3.

[7] Chen F, Song K, Hu B, Fan Y. Compact dual-band bandpass filter using HMSIW resonator and slot perturbation. IEEE Microwave and Wireless Components Letters. 2014 Jul 30;24(10):686-8.

[8] Wattikornsirikul N, Konpang J, Tubtongdee S, Sirikham A. High-selectivity Dual-band Bandpass Filter By Utilizing Asymmetrical Stepped-impedance Resonator. UTK Research Journal. 2020; 14(2) :10-8,

[9] Wang JP, Wang BZ, Wang YX, Guo YX. Dual-band microstrip stepped-impedance bandpass filter with defected ground structure. Journal of Electromagnetic Waves and Applications. 2008 Jan 1;22(4):463-70.

[10] Chu QX, Chen FC. A compact dual-band bandpass filter using meandering stepped impedance resonators. IEEE Microwave and Wireless Components Letters. 2008 May 12;18(5):320-2.

[11] Tsai LC. Design of dual-band bandpass filters using stepped-impedance resonators. In2011 2nd International Conference on Artificial Intelligence, Management Science and Electronic Commerce (AIMSEC) 2011 Aug 8 (pp. 6602-6605). IEEE.

[12] Chen CF, Huang TY, Wu RB. Design of dual-and triple-passband filters using alternately cascaded multiband resonators. IEEE Transactions on Microwave Theory and Techniques. 2006 Aug 28;54(9):3550-8.

[13] Wong SW, Deng F, Wu YM, Lin JY, Zhu L, Chu QX, Yang Y. Individually frequency tunable dual-and triple-band filters in a single cavity. IEEE Access. 2017 Jun 26;5:11615-25.

[14] Cogollos S, Micó P, Vague J, Boria VE, Guglielmi M. New design methodology for multiband waveguide filters based on multiplexing techniques. In2017 IEEE MTT-S International Microwave Symposium (IMS) 2017 Jun 4 (pp. 741-744). IEEE.

[15] Zhu L, Mansour RR, Yu M. Triple-band dielectric resonator bandpass filters. In2017 IEEE MTT-S International Microwave Symposium (IMS) 2017 Jun 4 (pp. 745-747). IEEE.

[16] Song K, Fan M, Zhang F, Zhu Y, Fan Y. Compact triple-band power divider integrated bandpass-filtering response using short-circuited SIRs. IEEE Transactions on Components, Packaging and Manufacturing Technology. 2017 Apr 13;7(7):1144-50.

[17] Guan X, Peng Y, Liu H, Lei J, Ren B, Qin F, Wen P, Liu F, Liu Y. Compact triple-band high-temperature superconducting filter using coupled-line stepped impedance resonator. IEEE Transactions on Applied Superconductivity. 2016 Aug 12;26(7):1-5.

[18] Gómez-García R, Loeches-Sánchez R, Psychogiou D, Peroulis D. Multi-stub-loaded differential-mode planar multiband bandpass filters. IEEE Transactions on Circuits and Systems II: Express Briefs. 2017 Mar 28;65(3):271-5.

[19] Chen XP, Wu K, Li ZL. Dual-band and triple-band substrate integrated waveguide filters with Chebyshev and quasi-elliptic responses. IEEE Transactions on Microwave Theory and Techniques. 2007 Dec 6;55(12):2569-78.

[20] Tsai WL, Shen TM, Chen BJ, Huang TY, Wu RB. Triband filter design using laminated waveguide cavity in LTCC. IEEE Transactions on Components, Packaging and Manufacturing Technology. 2014 May 13;4(6):957-66.

[21] Wang S, Zhang D, Zhang Y, Qing L, Zhou D. Novel dual-mode bandpass filters based on SIW resonators under different boundaries. IEEE Microwave and Wireless Components Letters. 2016 Dec 23;27(1):28-30.

[22] Zhang YP, Sun M. Dual-band microstrip bandpass filter using stepped-impedance resonators with new coupling schemes. IEEE Transactions on Microwave Theory and Techniques. 2006 Oct 2;54(10):3779-85.

[23] Hong JS, Lancaster MJ. Microstrip filters for RF/microwave applications. John Wiley & Sons; 2004 Apr 7.